Mixed Convection in a Square Cavity Filled with Porous Medium with Bottom Wall Periodic Boundary Condition

Dr. Ihsan Y. Hussein
Professor
Department of Mechanical Engineering
College of Engineering - Baghdad University
E-mail: drihsan@uobaghdad.edu.iq

Dr. Luma F. Ali
Lecturer
Department of Mechanical Engineering
College of Engineering- Baghdad University
E-mail: luma.fadhil@yahoo.com

ABSTRACT

Transient mixed convection heat transfer in a confined porous medium heated at periodic sinusoidal heat flux is investigated numerically in the present paper. The Poisson-type pressure equation, resulted from the substituting of the momentum Darcy equation in the continuity equation, was discretized by using finite volume technique. The energy equation was solved by a fully implicit control volume-based finite difference formulation for the diffusion terms with the use of the quadratic upstream interpolation for convective kinetics scheme to discretize the convective terms and the temperature values at the control volume faces. The numerical study covers a range of the hydrostatic pressure head $\Delta h = 5\ mm$, $\Delta h = 10\ mm$, $\Delta h = 15\ mm$, $\Delta h = 20\ mm$, and $\Delta h = 30\ mm$), sinusoidal amplitude range of $250 \le q_w \le 1250\ W/m^2$ and time period values of $(30 - 120)s$. Numerical results show that the pressure contours lines are influenced by hydrostatic head variation and not affected with the sinusoidal amplitude and time period variation. It is found that the average Nusselt number decreases with time and pressure head increasing and decreases periodically with time and amplitude increasing. The time averaged Nusselt number decreases with imposed sinusoidal amplitude and cycle time period increasing.

Keywords: porous medium, mixed convection, square cavity, sinusoidal periodic heating, finite volume method.

الحمل المختلط في حيز مربع مملوء بوسط مسامي مع شروط حدية دورية على الجدار السفلي

الاستاذ الدكتور احسان يحيى حسين
قسم الهندسة الميكانيكية
كلية الهندسة/جامعة بغداد

المدرس لمى فاضل علي
قسم الهندسة الميكانيكية
كلية الهندسة/جامعة بغداد

الخلاصة

يقدم البحث الحالي دراسة نظرية لأنتقال الحرارة بالحمل المختلط العابر في حيز محدد وسط مسامي محصور و مشبع بالمائع و مسخن بفيض حراري دوري ذو دالة جيبية.تم حل معادلة بواسون للضغط, الناتجة من تعويض معادلة دارسي للزخم في معادلة حفظ الكتلة, بإستخدام تقنية الحجم المحدد. تم حل معادلة الطاقة بإستخدام الحجم المحكوم الضمني المبني على صيغة الفروق المحددة مع إستخدام نظام القانون التربيعي للأستكمال الداخلي لحركة الحمل الحراري لفك ارتباط الحدود المشتركة الحمل و قيم درجات الحرارة على حدود الحجم المحكوم. ان التحقق العددي قد غطى كل قيم الحمل المختلط, ($\Delta h = 5$ ملم, $\Delta h = 10$ ملم, $\Delta h = 15$ ملم, $\Delta h = 20$ ملم, and $\Delta h = 30$ ملم) و التردد الجيبي ذو المدى ($250 \le q_w \le 1250$ واط/م^2) و قيم الفترة الزمنية $(30 - 120)$ثانية.لقد أظهرت النتائج النظرية ان توزيع الضغط يتاثر بتغير الارتفاع الستاتي و لا يتأثر بتغير مدى الموجة الجيبية و الفترة الزمنية للموجة. لقد وجد ان ان معدل قيم نسلت تنخفض بزيادة الزمن و ارتفاع الضغط تنخفض بشكل دوري بزيادة الزمن و مدى الدالة الجيبية. ان المعدل الزمني لقيم نسلت تنخفض بزيادة كل من المدى و الفترة الزمنية للدورة.

1. INTRODUCTION

The involvement of both natural and forced convection, referred as mixed convection, in porous media has been an important topic because of its wide range of applications in engineering and science. Some of these applications include oil extraction, energy storage units and ground water hydrology. Early studies on convection in porous media were largely devoted to buoyancy-induced flows and forced convection. The interaction mechanisms between these two modes of convection was given very little attention. For mixed convection in confined porous medium, the fluid velocity required for forced convection is occurred from either porous enclosures with lid-driven, vented openings, suction / injection ports, vibrational obstructed cavities, or others. In the present work, the mixed convection is achieved by providing a hydrostatic pressure head through an inlet port, accordingly a forced convection condition is imposed inside the porous enclosure. Besides, the buoyancy forces of natural convection are introduced due to the temperature gradient of the bottom heated wall. Mainly, the problems of mixed convection in confined porous medium can be classified into two categories, first the type of mixed convection in confined porous medium with uniform boundary conditions while the second category involves mixed convection with non-uniform boundary conditions.

The volume averaged equations governing unsteady, laminar, mixed convection flow in a top lid driven two-dimensional square enclosure filled with a Darcian fluid-saturated uniform porous media in the presence of internal heat generation was investigated numerically employing the finite-volume approach by **Khanafer,** and **Chamkha, 1999**. Then, the laminar transport processesin a lid-driven two-dimensional square cavity filled with a water-saturatedporous medium was conducted numerically utilizing the alternating direct implicit algorithm by **Al-Amiri, 2000** and **Kandaswamy, et. al., 2008**. Also, **Khanafer,** and **Vafai, 2002**, by using the finite volume numerical approach, analyzed the double-diffusive mixed convection in a lid-driven square enclosure filled with a non-Darcian fluid-saturated porous medium. The numerical investigation utilizing the finite volume method for two-dimensional steady state mixed convection flow in a square vented cavity filled with fluid-saturated porous medium with an isothermal left vertical surface and remaining three walls perfectly insulated was studied by **Mahmud,** and **Pop, 2006**. Later, **Oztop, 2006,** presented numerically the combined convection heat transfer and the fluid flow due to the position of heaters in a partially heated lid-driven square enclosure filled with homogeneous and isotropic porous material. The problem of mixed convection in a driven square cavity packed with homogeneous and isotropic porous medium was studied with the lattice Boltzmann method by **Chai, et. al., 2007**. Subsequently, the finite element numerical method carried out by **Barna, et. al., 2008,** examined and explained the two-dimensional steady mixed convection flow in a square vented cavity filled with fluid-saturated porous medium with all walls are isothermal at constant temperature. Besides, **Vishnuvardhanarao,** and **Das, 2008** and **Kumar, et. al., 2009** considered two-dimensional, mixed convection flow in a square enclosure filled with a Darcian fluid-saturated uniform porous medium. The first study of vibration and buoyancy induced transient mixed convection in an open-ended obstructed cavity filled with a fluid-saturated porous medium was investigated by **Chung,** and **Vafai, 2010**. Furthermore, **Kumar,** and **Murthy, 2010** focused their attention on a problem of steady non-Darcy mixed convection inside a vertical square enclosure filled with fluid-saturated porous medium with multiple fluid injections at the bottom wall and multiple suctions at the top wall. Thus, forced convection is imposed by this combination of suction/injection flow conditions and free convection is induced by the hot and isothermal left vertical wall. Afterwards, **Muthtamilselvan, 2011,** examined numerically, by employing the finite volume method, the steady

state two-dimensional mixed convection flow and heat transfer in a two-sided lid-driven square cavity filled with heat generating porous medium. **Kumari,** and **Nath, 2011** carried out numerically the steady state two-dimensional mixed convection in a square cavity flow of a heat generating fluid in a lid-driven square cavity filled with a fluid-saturated non-Darcy porous medium. Mixed convection is also taken place because of the buoyancy- and shear-driven flow induced by a hot plate moving through the horizontal mid-plane of a rectangular enclosure filled with fluid-saturated porous medium. This problem governing equations were thereby solved numerically using the finite difference method by **Waheed, et. al., 2011**. Furthermore, **Oztop, et. al., 2012,** performed a numerical study to analyze the flow field and temperature distributions of steady state laminar mixed convection heat transfer in a square left vertical wall partially cooled lid-driven cavity filled with fluid-saturated porous medium.

For the second category of mixed convection with non-uniform boundary conditions, The numerical study to obtain combined convection field in an inclined lid-driven enclosures filled with fluid-saturated porous media and heated from one wall with a non-uniform heater was carried out by **Oztop,** and **Varol, 2009**. They assumed that the lid is moving at constant speed and temperature while the bottom wall of the cavity has sinusoidal temperature distribution and remaining walls are adiabatic. Thence, the characteristics of a two-sided lid-driven mixed convection flow in a steady state two-dimensional square cavity filled with heat generating porous medium was numerically inspected by **Muthtamilselvan, et. al., 2010**. The top wall is maintained at a constant temperature and the bottom wall is sustained at uniform or non-uniform temperatures (sinusoidal type), while the side vertical walls were considered to be adiabatic. Detailed analysis of mixed convection of fluid within square porous cavity with generalized boundary conditions involving linear and uniform heating of adjacent walls or uniform cooling of a side wall in presence of uniform motion of top adiabatic wall and uniform heating of the bottom cavity wall was carried numerically by **Basak, et. al., 2010**. Then, **Basak, et. al., 2011** performed a penalty finite element method to analyze the influence of various walls thermal boundary conditions on mixed convection lid-driven flows in a square cavity filled with fluid-saturated porous medium. Thereafter, the influence of uniform and non-uniform heating of the bottom wall on the flow and heat transfer characteristics due to lid-driven mixed convection flow within a square cavity filled with porous medium was studied numerically utilizing penalty finite element analysis by **Basak, et. al., 2012**. Furthermore, **Ramakrishna, et. al., 2012,** explored the numerical study that deals with lid-driven mixed convection within square cavity filled with porous media for various thermal boundary conditions based on thermal aspect ratio on bottom and side walls where the top wall is adiabatic and moves from left to right with uniform velocity. The influence of the non-uniform thermal boundary conditions on mixed convection flow and heat transfer in a lid-driven cavity filled with fluid-saturated porous medium was investigated numerically by **Sivasankaran,** and **Pan, 2012**.

In the present study, transient mixed convection in a two-dimensional square cavity subjected to static pressure head and filled with a Darcian fluid-saturated porous medium is investigated numerically. The two vertical walls of the confined porous medium are insulated while the bottom wall is heated periodically and the heat is lost by convection from the top wall which is exposed to the environment. Detailed numerical solutions are carried out by utilizing the finite volume method for a range of parameters, namely the pressure head, amplitude, time period of sinusoidal imposed heat flux. Numerical results are obtained for pressure, and temperature fields within the enclosure and are displayed using pressure contours lines and isotherms respectively. Also, the average and time averaged Nusselt number variations are depicted in the present paper.

2. MATHEMATICAL FORMULATION

The two-dimensional inclined cavity under investigation is filled with fluid-saturated porous medium and all the walls are impermeable except the upper wall. Glass beads with specified diameter is used as a porous media and distilled water is used as the incompressible fluid that saturates the porous medium. The schematic configuration of the problem is illustrated in **Fig. 1**, with L denoting the length of the square cavity. Furthermore, the porous medium is assumed to be in local thermal equilibrium with the fluid.

The two vertical left and right sidewalls are adiabatic, and a periodic sinusoidal heating is applied on the bottom wall while the top wall is exposed to the environment and losses heat by natural convection. Water is supplied to the cavity from an external tank with a static head from an opening inlet at the bottom left corner and there is a water outlet open at the upper right corner. The thermophysical properties of the fluid and the porous material are taken to be constant except for the density variation in the buoyancy force, which is treated by the Boussinesq approximation.

The Darcy equation formulation is adopted for modeling the fluid flow in the porous medium. The governing equations for mass, momentum, and energy in two-dimensional, Cartesian coordinates, laminar flow are as follows:

Continuity equation

$$\frac{\partial u}{\partial x}+\frac{\partial v}{\partial y}=0 \tag{1}$$

Momentum equation

$$u=-\frac{K}{\mu_f}\left[\frac{\partial p}{\partial x}+\rho_f g\sin\varphi\right] \tag{2}$$

$$v=-\frac{K}{\mu_f}\left[\frac{\partial p}{\partial y}+\rho_f g\cos\varphi\right] \tag{3}$$

Energy equation

$$\sigma\frac{\partial T}{\partial t}+\left[u\frac{\partial T}{\partial x}+v\frac{\partial T}{\partial y}\right]=\frac{k_{eff}}{(\rho C_p)_f}\left[\frac{\partial^2 T}{\partial x^2}+\frac{\partial^2 T}{\partial y^2}\right] \tag{4}$$

where u and v are the fluid velocities in x and y directions respectively, K is the porous medium permeability, μ_f is the fluid dynamic viscosity, p is fluid pressure, ρ_f is the fluid density, g is the acceleration due to gravity, φ is the inclination angle of the cavity, T is the fluid temperature, t is the time, and σ is the specific heat ratio which is given as:

$$\sigma=\frac{(\rho C_p)_m}{(\rho C_p)_f} \tag{5}$$

where C_p is the specific heat at constant pressure and the subscripts m and f denoted to effective value and fluid phase respectively, k_{eff} is effective thermal conductivity of porous medium and it is given by **Hadley, 1986**:

$$\frac{k_{eff}}{k_f} = (1-\alpha_o)\frac{\varepsilon f_o + \lambda(1-\varepsilon f_o)}{1-\varepsilon(1-f_o)+\lambda\varepsilon(1-f_o)} + \alpha_o \frac{2\lambda^2(1-\varepsilon)+(1+2\varepsilon)\lambda}{(2+\varepsilon)\lambda+1-\varepsilon} \quad (6)$$

where ε is the porosity of the porous medium and k_s and k_f are the thermal conductivity of the solid material and fluid phase of the porous medium respectively, $\lambda = k_s/k_f$is the thermal conductivity ratio of solid and liquid phases, $f_o$is a parameter which is expected to be approximately constant for a contiguous solid, and $\alpha_o$is an another parameter that is very sensitive to porosity changes and it is represented for different porosity ranges as, **Suresh, et. al., 2005**:

$$\log \alpha_o = -4.898\varepsilon \qquad 0 \le \varepsilon \le 0.0827 \quad (7a)$$

$$\log \alpha_o = -0.405 - 3.154(\varepsilon - 0.0827) \qquad 0.0827 \le \varepsilon \le 0.298 \quad (7b)$$

$$\log \alpha_o = -1.084 - 6.778(\varepsilon - 0.298) \qquad 0.298 \le \varepsilon \le 0.58 \quad (7c)$$

The equation of state under the Boussinesq approximation is assumed to be:

$$\rho = \rho_o[1 - \beta(T - T_o)] \quad (8)$$

where ρ_o and T_o are respectively the density and the temperature in the reference state, β the coefficient of thermal expansion.
In accordance with the present problem, the above governing equations are subjected to the following initial and boundary conditions:

$$u = v = 0,\ T = T_o \qquad \text{at} \quad t = 0 \quad (9)$$

$$u = v = 0,\ \frac{\partial T}{\partial x} = 0 \qquad \text{at} \quad x = 0 \ \text{and} \ x = L \quad (10)$$

$$u = 0,\ k_{eff}\frac{\partial T}{\partial y} = q_o + a\sin(2\pi t/\tau),\ p = \rho g(L + \Delta h) \qquad \text{at} \quad y = 0 \quad (11)$$

$$u = 0,\ k_{eff}\frac{\partial T}{\partial y} = h(T - T_o),\ p = 0 \qquad \text{at} \quad y = L \quad (12)$$

where q_o is the uniform heat flux, a is the sinusoidal amplitude, h is the natural heat convection coefficient.
After inserting the Boussinesq approximation in the momentum **Eqs. (2)** and **(3)**, and the resulting equations substituted in **Eq. (1)**, the following new pressure differential equation is obtained:

$$\frac{\partial^2 p}{\partial x^2} + \frac{\partial^2 p}{\partial y^2} = g\rho_o\beta\left[\sin\varphi\frac{\partial T}{\partial x} + \cos\varphi\frac{\partial T}{\partial y}\right] \quad (13)$$

Eqs. (4) and **(13)** are solved numerically with the applied initial and boundary conditions to simulate the mixed convection in the inclined square cavity. The average Nusselt number on the bottom hot wall is given as:

$$Nu = \frac{\int_0^L \frac{\partial T}{\partial y} dx}{(T_b - T_o)} \tag{14}$$

where T_b is the boom hot wall temperature.
The time averaged Nusselt number for specific time period τ is casted as;

$$Nu_{\tau av} = \frac{1}{\tau} \int_{(r-1)\tau}^{r\tau} \left[\frac{-\int_0^L \frac{\partial T}{\partial y}\Big|_{y=0} dx}{L(T_b - T_0)} \right] d\tau \tag{15}$$

where r is the number of time period.

3. NUMERICAL FORMULATION

The governing **Eqs. (4)** and **(13)** in the present problem of mixed convection in a cavity filled with porous medium are solved by using the finite volume method **Versteeg,** and **Malalasekera, 2007**. A fully implicit scheme is applied for discretizing the time derivatives. The convective fluxes at the cell interface are discretized by employing the Quadratic Upwind Interpolation for Convective Kinematics (QUICK) scheme and a second-order central difference scheme is used for the diffusion terms. The resulting algebraic equations are solved by the tri-diagonal matrix algorithm (TDMA). For convergence criteria, the relative variations of the temperature and pressure between two successive iterations are demanded to be smaller than the previously specified accuracy levels of 10^{-5}. The iterative procedure is initiated by the solution of the pressure equation followed by calculating the velocity field and then solving the energy equation until reaching a specific temperature. This specified temperature is the mean value of selected location temperatures near the bottom heated wall. In the present study, the desired temperature is taken as $90\,℃$ which is the temperature at which the working water fluid changes to the two phase condition.
Before proceeding further, the grid independency tests are performed first. Numerical experiments were performed for various grid sizes viz. 12×12, 16×16, 20×20, 24×24, 28×28, and 32×32 to test and estimate the grid independent solutions. These numerical experiments were accomplished for a hydrostatic head $\Delta h = 10\,mm$ and constant heat flux $q = 500\ W/m^2$. It is observed that the average Nusselt number values at the bottom heated wall of the enclosure are very near to each other when the grid size is near 24×24. Therefore, a grid size of 24×24 is chosen for further computations because it consumed less computing time. The parameters of convergence are fixed to 10^{-5} for both pressure and temperature. Furthermore, a similar test was done for the time step value and it is found that $\Delta t = 0.05\ sec$ is very sufficient for the present problem.

4. RESULTS AND DISCUSSION

Published experimental data are not available for the cavity configuration and boundary conditions similar to that taken in the present study. Thus, the validation of the computations against suitable experimental data could not be performed. However, in order to validate the predictive capability and accuracy of the present code, three published works have been chosen. For validation purpose of mixed convection flow and heat transfer, a differentially heated square cavity of natural laminar heat transfer is considered. The left surface is heated isothermally and right surface is cooled to a

lower temperature with top and the bottom walls maintained thermally insulated. Average Nusselt number is calculated and depicted in **Table 1** for $Ra = 100$ and compared with the earlier investigations **Saeid,** and **Pop, 2004**, **Baytas, 2000**, and **Walker,** and **Homsy, 1978**. From **Table 1**, it is clearly revealed that the agreement between the present and the previous results is very good indeed. So, these results provide great confidence to the accuracy of the present numerical method.

In the present investigation, Soda Lime glass beads saturated with distilled water is chosen as a porous media. Its permeability and porosity are taken as 1.57×10^{-9} and 0.418 respectively. The controlling parameters on the heat transfer and fluid flow for this investigation are the hydrostatic pressure head and sinusoidal amplitude and time period. The computations have been carried out for the pressure head of $\Delta h = 10$and $20mm$. The sinusoidal amplitude is varied in the range from 250 to $1250\ W/m^2$ while the time period range is 30–120 s.

The pressure field is indicated in **Fig. 2** for hydrostatic pressure head values of $\Delta h = 10\ mm$ and $\Delta h = 20\ mm$ and a fixed value of $a = 750\ W/m^2$ amplitude and $\tau = 60\ s$ sinusoidal time period. It is clear from this figure that the pressure values at specific nodal point increases as the pressure head difference. Also, the pressure distribution is not affected by the variation of the amplitude and the time period as seen in **Fig. 3**. This figure is plotted for different amplitudes and time period of $\tau = 30\ s$ and pressure head value of $\Delta h = 20\ mm$. The pressure is unaffected because the temperature gradient is small value that is deduced from the amplitude value and taken place in the right hand side of **Eq. (13)** compared with the pressure value on the bottom boundary wall.

The steady state response of the periodic sinusoidal boundary condition is performed when the absolute difference of time averaged Nusselt number between two successive periodic cycles is less than an estimated number of 0.35. When this state response is reached, the temperature contours line for eight time steps of the last cycle is demonstrated for specific amplitude value of $a = 500\ W/m^2$, cycle time period of $\tau = 60s$, and three hydrostatic pressure head values of $\Delta h = 10\ mm$ and $\Delta h = 20\ mm$, in **Figs. 4** and **5** respectively. It can be noticed that the first half of the cycle is almost devoted to the temperature increasing of the bottom wall and the nearby porous domain. While the second half of the cycle is adapted to the convection heat transfer to the downstream of the porous enclosure and the bottom temperature is approximately remaining constant during this half of the heating periodic cycle. In the second half of the cycle, the imposed heat flux becomes small and not sufficient to increase the bottom temperature but just to maintain its temperature almost constant. On the other hand, there is a temperature difference between the bottom region and the upper region of the confined porous medium which tends to a buoyancy effect inducing through the domain and hence natural convection currents are invoked in addition to the mixed convection and liquid velocity effect in transferring heat through the cavity. Also, it is clear that the mixed convection influence increases with the pressure head difference increase from $10\ mm$ to $20\ mm$ and results in a higher temperature values as shown in **Figs. 4** and **5** respectively.

Figs. 6 to **8** present the influence of the amplitude variation from $250\ W/m^2$ to $750\ W/m^2$on the temperature field within the eight time steps of the last cycle when a steady state response is reached for the case of $10mm$ pressure head and $30s$ time period. It can be easily seen that the increase of the amplitude tends to temperature increase especially for higher amplitude values that leads to vigorous increase in temperature distribution. The main reason behind this behavior is that the temperature difference in the porous domain increases when the imposed amplitude is increased and consequently the buoyancy force effect is increased. This tends to convection currents increasing and obtaining higher temperature values. Furthermore, the influence of time period on the

temperature contours line is observed in **Figs. 9** and **10** for hydrostatic pressure head of $20mm$ and imposed heat flux amplitude of $250\,W/m^2$. These figures pronounce that the time period increase causes a temperature increasing near the bottom wall because the time of heating operation increases and thus more heat flux amplitude is imposed to the porous enclosure. Additionally a further time is given to transfer the heat of the bottom region to the entire porous domain region when the time period is increased and this leads to heating most of the domain by the superposition of forced and natural convection mechanism caused by pressure head difference and buoyancy force effects respectively.

The variation of the average Nusselt number is plotted with consumed time of sinusoidal imposed heating on the bottom wall of a non-inclined porous enclosure in **Figs. 11** and **12** for $\Delta h = 10\,mm$ and $\Delta h = 20\,mm$ hydrostatic pressure head difference respectively. This figure is displayed for various values of amplitude from $250\ W/m^2$to $750\ W/m^2$, time period of $60\,s$ and $30\ s$successively. It can be easily seen that the Nusselt number decreases periodically with heating time increasing. By referring to **Eq. (14)**, this decrease is mainly due to the fact that the Nusselt number is inversely proportional with the temperature difference between the bottom heated wall and the downstream liquid temperature. Therefore, as this temperature difference increases with time increasing, the Nusselt number is decreased and has a periodic behavior because of the periodicity of the imposed heat flux. Additionally, the average Nusselt number is not altered with the amplitude increasing at certain simulation time because the mixed convection currents accelerates the heating process and has vigorous effect on the heat transfer characteristics compared with the buoyancy force influence that is resulted from the temperature gradient related mainly to the imposed amplitude heat flux.

Moreover, the variation of average Nusselt number with periodic sinusoidal heating time along the enclosure bottom wall at different response time period is presented in **Figs. 13** and **14** for hydrostatic pressure head values of $10\,mm$ and $20\,mm$ respectively. From these two figures, it is indicated that the peak value of Nusselt number for each time period case decreases with time period increasing. The temperature difference between the heated wall and the top region of the enclosure increases with the time period increasing because there is sufficient time for heating process. This is thought to be the reason behind the reduction of the Nusselt number with increasing time period because of the contrary relation between the Nusselt number and the mentioned temperature difference. For the same reason mentioned previously for the average Nusselt number, the time averaged Nuselt number during the cycle of steady state response decreases with the increasing of both the imposed sinusoidal amplitude and the cycle time period as demonstrated in **Figs. 15** and **16** for hydrostatic pressure head values of $10\,mm$ and $20\,mm$ successively.

5. CONCLUSIONS

Convective flow and heat transfer in a square porous cavity with sinusoidal periodic heat flux at the bottom wall is investigated numerically. The following conclusions are made from this study.

- The pressure field and the velocity vector are increased with increasing hydrostatic pressure head.
- The first sinusoidal heating half cycle is devoted to the bottom wall and nearby porous domain temperature increasing while the second half of the cycle is adapted to convection heat transfer to the porous domain downstream.

- The amplitude increase causes temperature increase especially for higher amplitude values that leads to vigorous increase in temperature distribution and the sinusoidal time period heating increase causes a temperature increasing near the bottom wall.
- The average Nusselt number decreases periodically with sinusoidal heating time increasing for certain amplitude value and also decreases with amplitude increasing for specific simulation time when the pressure head is zero but it is not altered with amplitude increasing when the head pressure is greater than zero.
- The peak value of the average Nusselt number decreases with time increasing for each time period case.
- The time averaged Nusselt number decreases with the increasing of the imposed sinusoidal amplitude and the cycle time period.

REFERENCES

Al-Amiri, A. M., 2000, *Analysis of Momentum and Energy Transfer in a Lid-Driven Cavity Filled with a Porous Medium*, Int. J. Heat Mass Transfer, Vol. 43, pp. 3513–3527.

Basak, T., Krishna Pradeep, P. V., Roy, S., and Pop, I., 2011, *Finite Element Based Heat line Approach to Study Mixed Convection in a Porous Square Cavity with Various Wall Thermal Boundary Conditions*, Int. J. Heat Mass Transfer, Vol. 54, pp. 1706-1727.

Basak, T., Roy, S., and Chamkha, A. J., 2012, *A Peclet Number Based Analysis of Mixed Convection for Lid-Driven Porous Square Cavity with Various Heating of Bottom Wall*, Inter. Commun. Heat and Mass Transfer, Vol. 39, pp. 657-664.

Basak, T., Roy, S., Singh, S. K., and Pop, I., 2010, *Analysis of Mixed Convection in a Lid-Driven Porous Square Cavity with Linearly Heated Side Wall(s)*, Int. J. Heat Mass Transfer, Vol. 53, pp. 1819-1840.

Barna, S. F., Bhuiyan, A. A., Banna, M. H., and Sadrul Islam, A. K. M., 2008, *Effect of Inlet to Cavity Width Ratio on Mixed Convection in a Microstructure Filled Vented Cavity*, Proc. of the 4th BSME-ASME Int. Conf. on Thermal Engineering, Dhaka, Bangladesh, pp. 48-55.

Baytas, A. C., 2000, *Entropy Generation for Natural Convection in an Inclined Porous Cavity*, Int. J. Heat Mass Transfer, Vol. 43, pp. 2089–2099.

Chai, Z., Guo, Z., and Shi, B., 2007, *Lattice Boltzmann Simulation of Mixed Convection in a Driven Cavity Packed with Porous Medium*, Computational Science – ICCS 2007, Lecture Notes in Computer Science, Vol. 4487, pp. 802-809.

Chung, S., and Vafai, K., 2010, *Vibration Induced Mixed Convection in an Open-Ended Obstructed Cavity*, Int. J. Heat Mass Transfer, Vol. 53, pp. 2703-2714.

Hadley, G. R., 1986, *Thermal Conductivity of Packed Metal Powder*, Inter. J. Heat and Mass Transfer, Vol. 29, No. 6, pp. 909-920.

Kandaswamy, P., Muthtamilselvan, M., and Lee, J., 2008, *Prandtl Number Effects on Mixed Convection in a Lid-Driven Porous Cavity*, J. Porous Media Vol. 11, pp. 791–801.

Khanafer , K. M. and Chamkha , A. J., 1999, *Mixed Convection Flow in a Lid-Driven Enclosure Filled with a Fluid-Saturated Porous Medium*, Inter. J. Heat Mass Transfer, Vol. 42, pp. 2465–2481.

Khanafer, K., and Vafai, K., 2002, *Double-Diffusive Mixed Convection in a Lid-Driven Enclosure Filled with a Fluid-Saturated Porous Medium*, Numer. Heat Transfer, Part A, Vol. 42, pp. 465–486.

Kumar, B. V., and Murthy, S.V.S.S.N.V.G. K., 2010, *Mixed Convection in a Non-Darcian Fluid Saturated Square Porous Enclosure Under Multiple Suction Effect*, Int. J. Heat Mass Transfer, Vol. 53, pp. 5764–5773.

Kumar, D. S., Das, A. K., and Dewan, A., 2009, *Analysis of Non-Darcy Models for Mixed Convection in a Porous Cavity Using a Multigrid Approach*, Numer. Heat Transf. Part A, Vol. 56, pp. 685–708.

Kumari, M. and Nath, G., 2011, *Steady Mixed Convection Flow in a Lid-Driven Square Enclosure Filled with a Non-Darcy Fluid Saturated Porous Medium with Internal Heat Generation*, J. Porous Media, Vol. 14, No. 10, pp. 893 – 905.

Mahmud, S., and Pop, I., 2006, *Mixed Convection in a Square Vented Enclosure Filled with a Porous Medium*, Inter. J. Heat Mass Transfer, Vol. 49, pp. 2190–2206.

Muthtamilselvan, M., 2011, *Forced Convection in a Two-Sided Lid-Driven Cavity Filled with Volumetrically Heat-Generating Porous Medium*, Int. J. Appl. Math. And Mech., Vol. 7, No. 13, pp. 1–16.

Muthtamilselvan, M., Das, M. K., and Kandaswamy, P., 2010, *Convection in a Lid-Driven Heat-Generating Porous Cavity with Alternative Thermal Boundary Conditions*", Transp. Porous Med., Vol. 82, pp. 337–346.

Oztop, H. F., 2006, *Combined Convection Heat Transfer in a Porous Lid-Driven Enclosure Due to Heater with Finite Length*, Int. Community. Heat Mass Transf., Vol. 33**,** pp.772–779.

Oztop, H. F., and Varol, A., 2009, *Combined Convection in Inclined Porous Lid-Driven Enclosures with Sinusoidal Thermal Boundary Condition on One Wall*, Progress in Computational Fluid Dynamics, Vol. 9, No. 2, pp. 127–131.

Oztop, H. F., Varol, Y., Pop, I., and Al-Saleem, K., 2012, *Mixed Convection in Partially Cooled Lid-Driven Cavity with a Non-Darcy Porous Medium*, Progress in Computational Fluid Dynamics, Vol. 12, No. 1, pp. 46–55.

Ramakrishna, D., Basak, T., Roy, S., and Pop, I., 2012, *Numerical Study of Mixed Convection within Porous Square Cavities Using Bejan's Heatlines: Effects of Thermal Aspect Ratio and Thermal Boundary Conditions*", Inter. J. Heat and Mass Transfer, Vol. 55, pp. 5436–5448.

Sivasankaran, S., and Pan, K. L., 2012, *Numerical Simulation on Mixed Convection in a Porous Lid-Driven Cavity with Non-uniform Heating on Both Side Walls*", Numer. Heat Trans. Part A, Vol. 61, pp. 101–121.

Saeid, N. H., and Pop, I., 2004, *Transient Free Convection in a Square Cavity Filled with a Porous Medium*, Int. J. Heat Mass Transfer, Vol. 47, pp. 1917–1924.

Suresh, Ch. S. Y., VamseeKriskna, Y., Sundararajan, T., and Das, S. K., 2005, *Numerical Simulation of Three-Dimensional Natural Convection Inside a Heat Generating Anisotropic Porous Medium*, J. Heat Mass Transfer, Vol. 41, pp. 799–809.

Versteeg H. K., and Malalasekera, W., 2007, *An Introduction to Computational Fluid Dynamics: the Finite Volume Method*, 2nd Edition, Pearson Education Limited Prentice Hall, England.

Vishnuvardhanarao, E., and Das, M. K., 2008, *Laminar Mixed Convection in a Parallel Two-Sided Lid-Driven Differentially Heated Square Cavity Filled with Fluid-Saturated Porous Medium*, Numer. Heat Transf. Part A, Vol. 53, pp. 88–110.

Waheed, M. A., Odewole, G. A., and Alagbe, S. O., 2011, *Mixed Convective Heat Transfer in Rectangular Enclosures Filled with Porous Media*", ARPN J. of Eng. & Applied Sciences, Vol. 6, No. 8, pp. 47–60.

Walker, K. L., and Homsy, G. M., 1978, *Convection in a Porous Cavity*, J. Fluid Mech. Vol. 87, pp. 449–474.

Table 1. Comparison of average Nusselt number with previous workers for $Ra = 100$.

Authors	Nu
Saeid and Pop, 2004	3.002
Baytas, 2000	3.160
Walker and Homsy, 1978	3.097
Present result	3.076

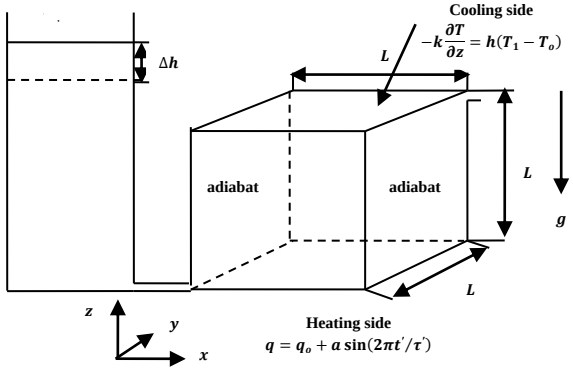

Figure 1. Schematic diagram of the physical problem and coordinates system.

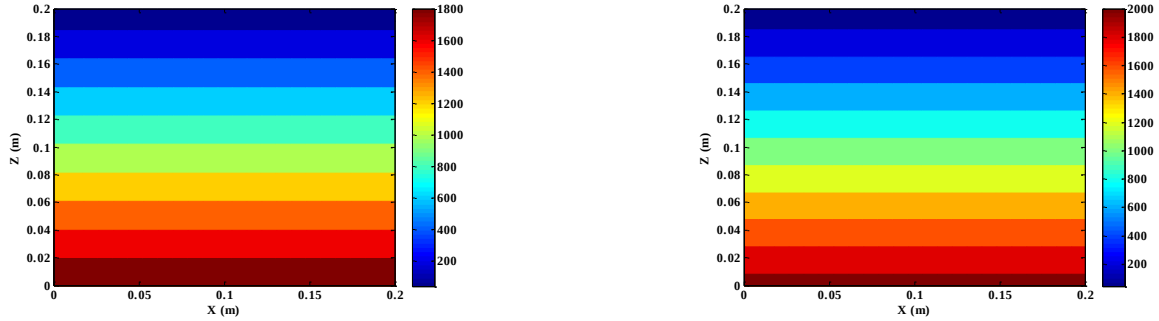

(a) (b)

Figure 2. Pressure field with $a = 750\,W/m^2$and $\tau = 60s$: (a) $\Delta h = 10mm$, (b) $\Delta h = 20mm$.

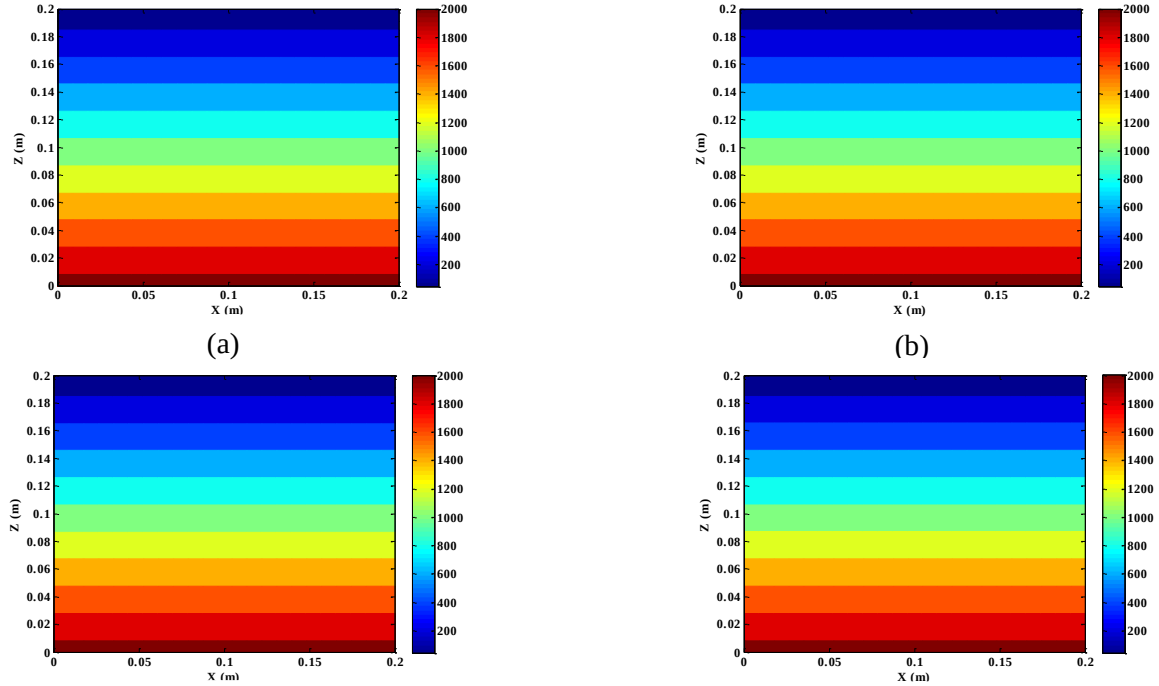

(a) (b)

(c) (d)

Figure 3. Pressure contours line for different amplitude values with $\Delta h = 20\ mm$ and $\tau = 30\ s$: (a) $250\ W/m^2$, (b) $375\ W/m^2$, (c) $500\ W/m^2$, (d) $750\ W/m^2$.

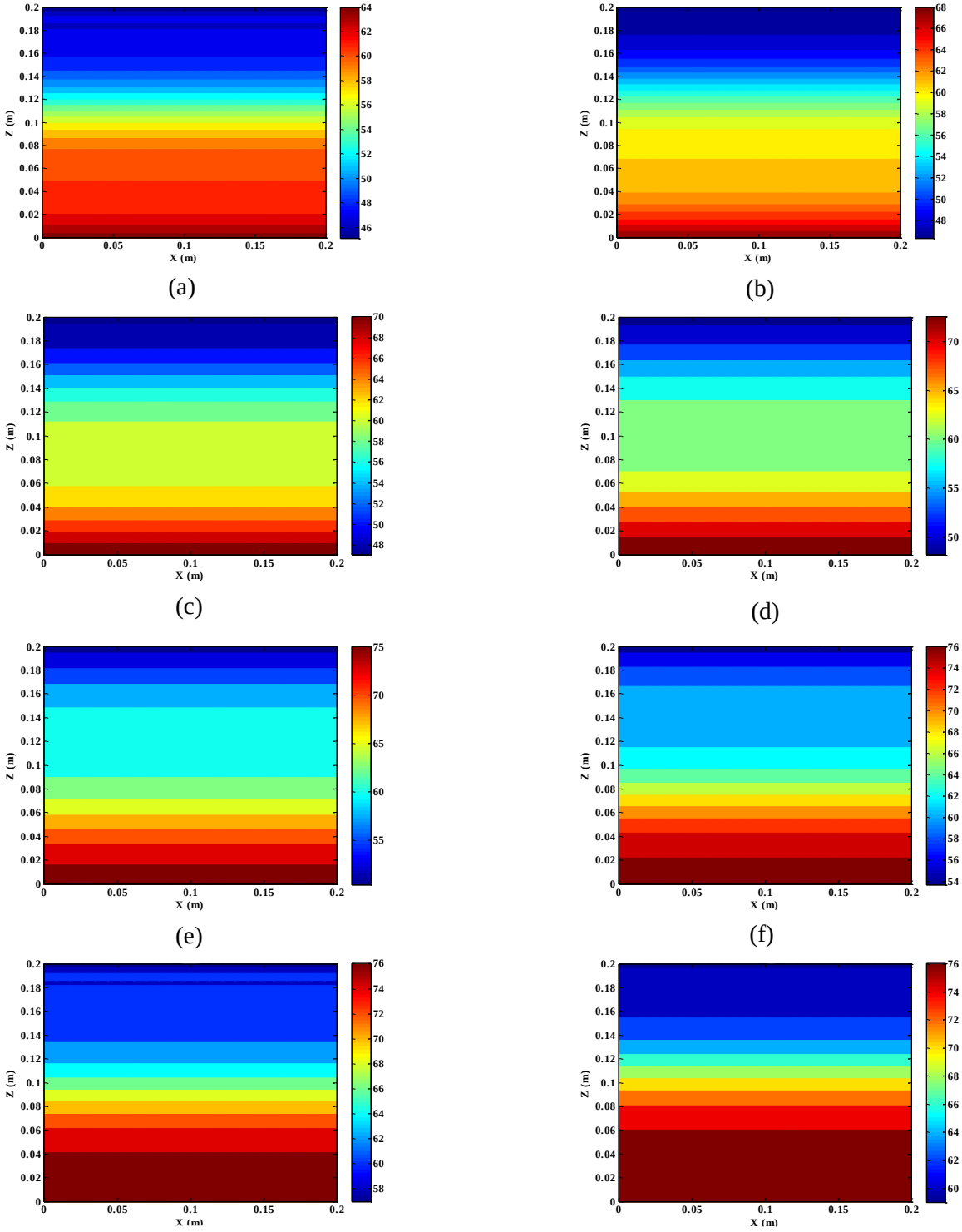

Figure 4. Temperature distribution for different time step when reaching steady state response with $a = 500\ W/m^2$, $\tau = 60s$, and $\Delta h = 10\ mm$: (a) $t = 0.125\ \tau$, (b) $t = 0.25\ \tau$, (c) $t = 0.375\ \tau$ (d) $t = 0.5\ \tau$, (e) $t = 0.625\ \tau$, (f) $t = 0.75\ \tau$, (g) $t = 0.875\ \tau$, (h) $t = \tau$.

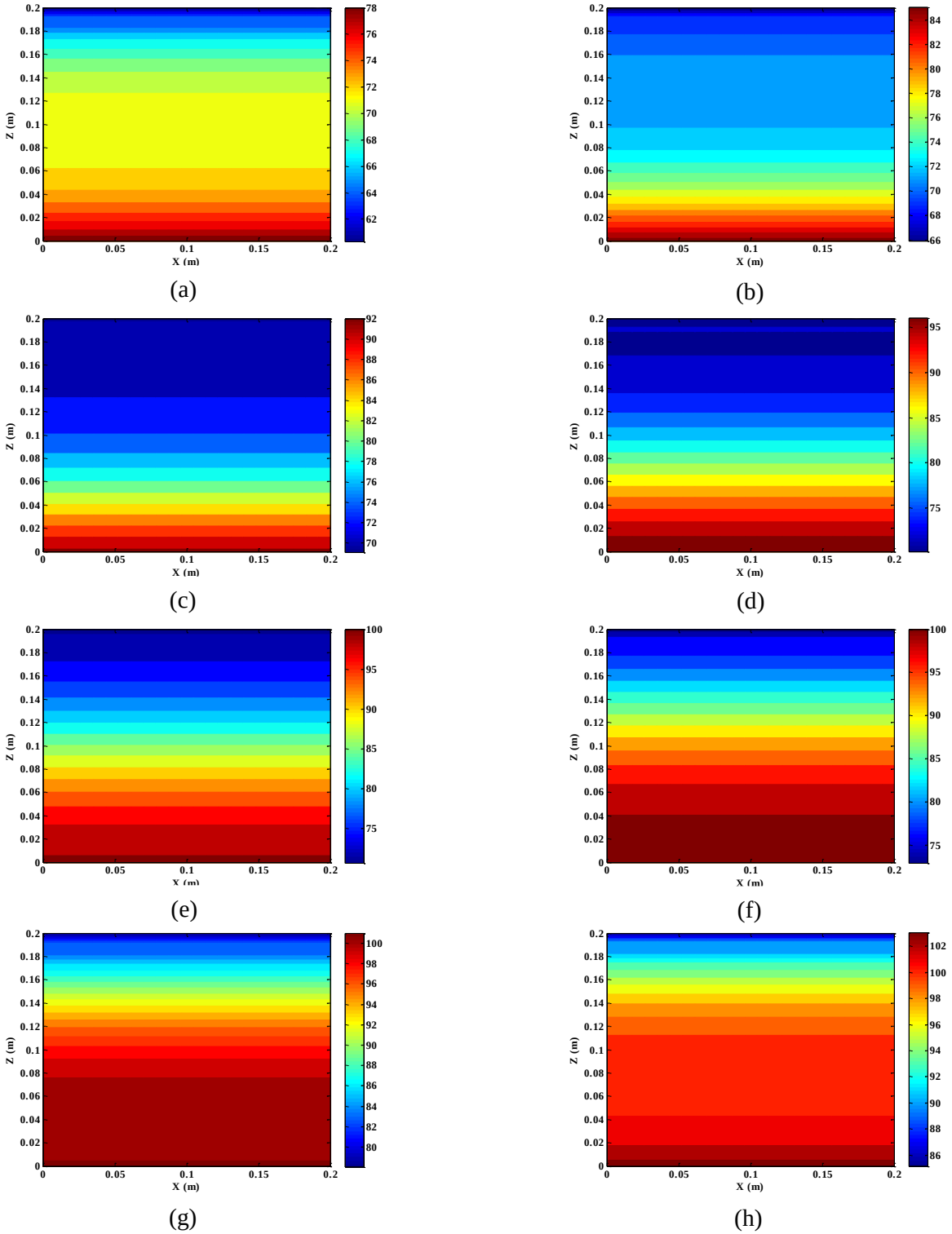

Figure 5. Temperature distribution for different time step when reaching steady state response with $a = 500\ W/m^2$, $\tau = 60s$, and $\Delta h = 20mm$: (a) $t = 0.125\ \tau$, (b) $t = 0.25\ \tau$, (c) $t = 0.375\ \tau$ (d) $t = 0.5\ \tau$, (e) $t = 0.625\ \tau$, (f) $t = 0.75\ \tau$, (g) $t = 0.875\ \tau$, (h) $t = \tau$.

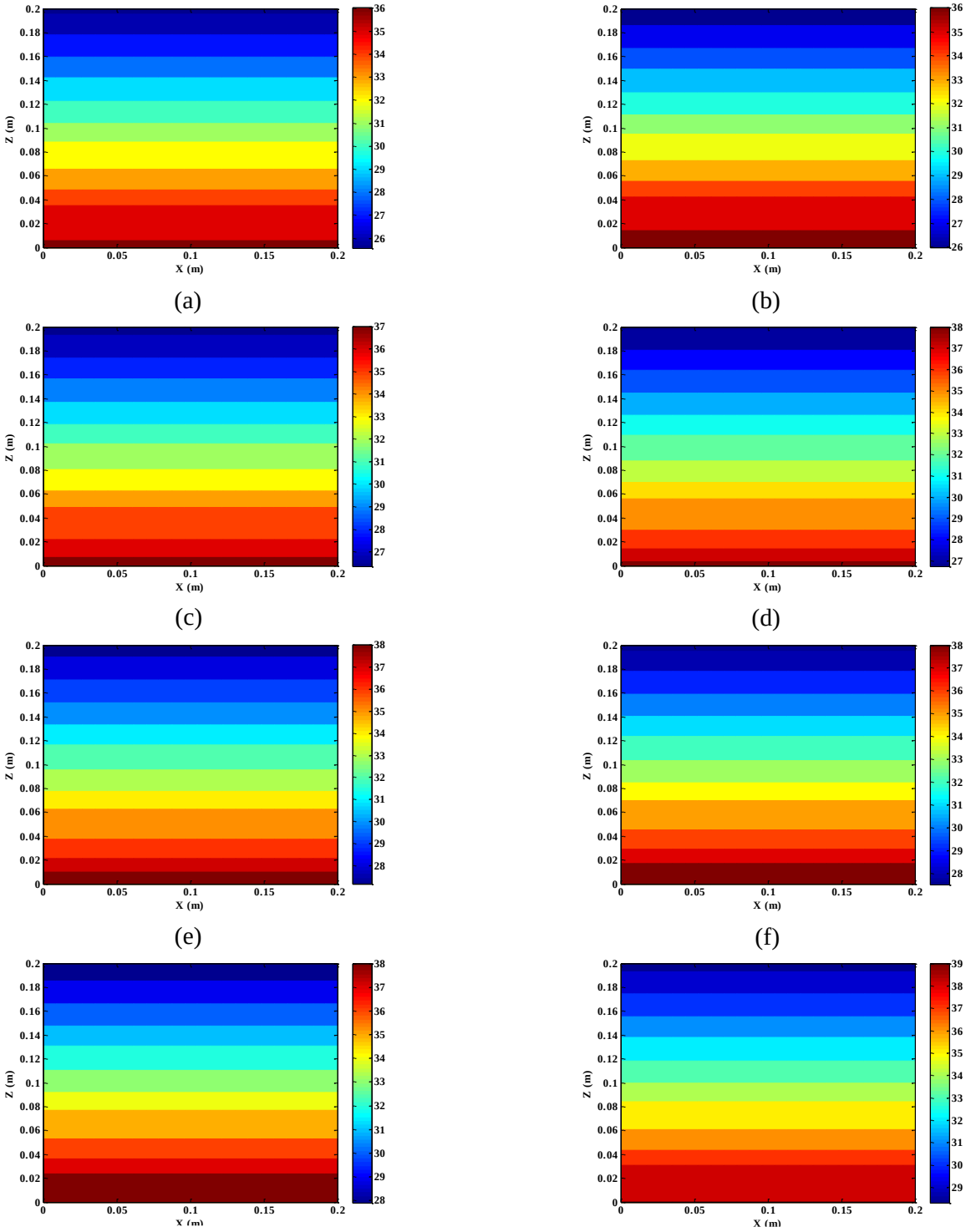

Figure 6. Temperature contours line for different time step when reaching steady state response with $a = 250\ W/m^2$, $\tau = 30s$, and $\Delta h = 10mm$: (a) $t = 0.125\tau$, (b) $t = 0.25\tau$, (c) $t = 0.375\tau$ (d) $t = 0.5\tau$, (e) $t = 0.625\tau$, (f) $t = 0.75\tau$, (g) $t = 0.875\tau$, (h) $t = \tau$.

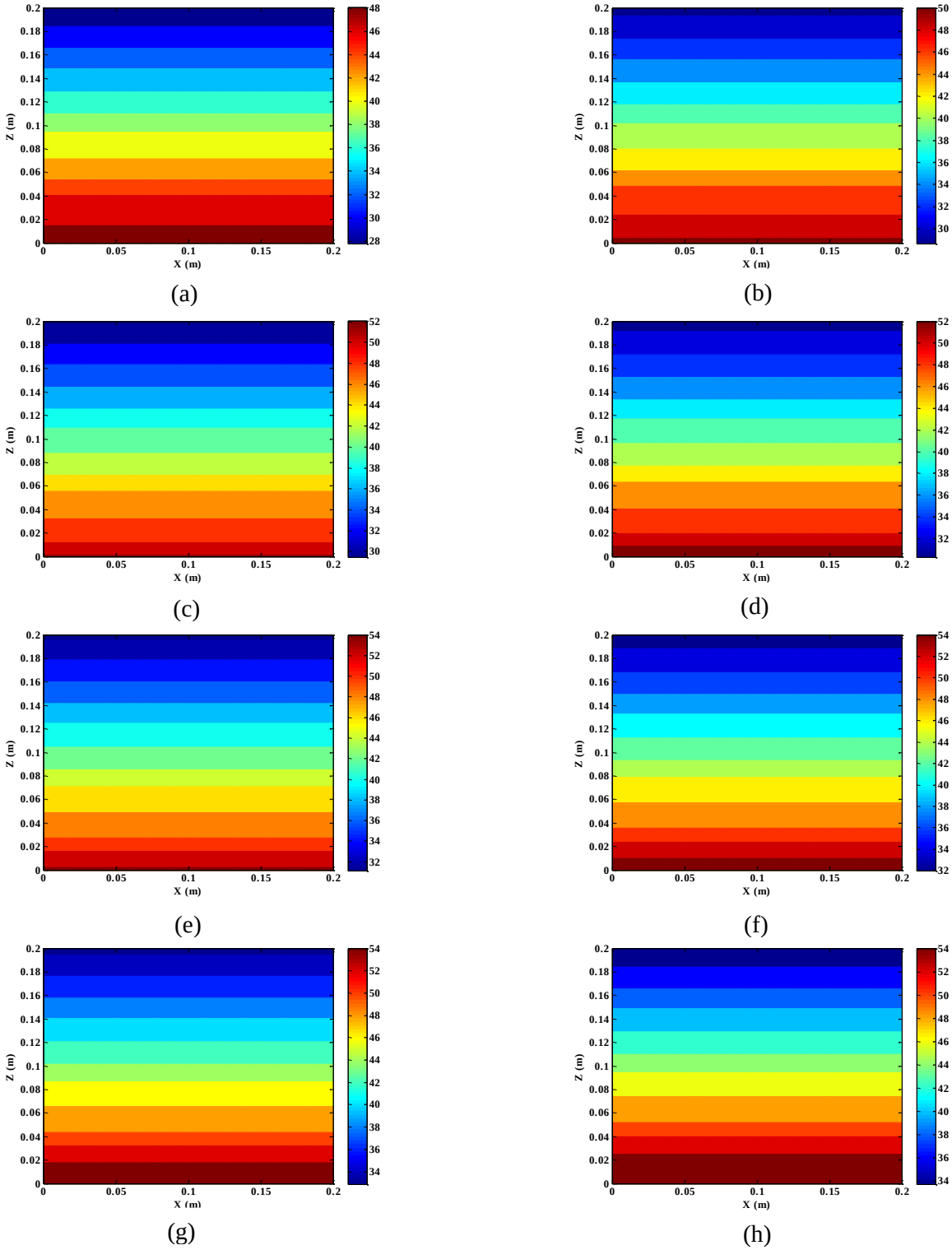

Figure 7. Temperature contours line for different time step when reaching steady state response with $a = 500\ W/m^2$, $\tau = 30s$, and $\Delta h = 10mm$: (a) $t = 0.125\tau$, (b) $t = 0.25\tau$, (c) $t = 0.375\tau$ (d) $t = 0.5\tau$, (e) $t = 0.625\tau$, (f) $t = 0.75\tau$, (g) $t = 0.875\tau$, (h) $t = \tau$.

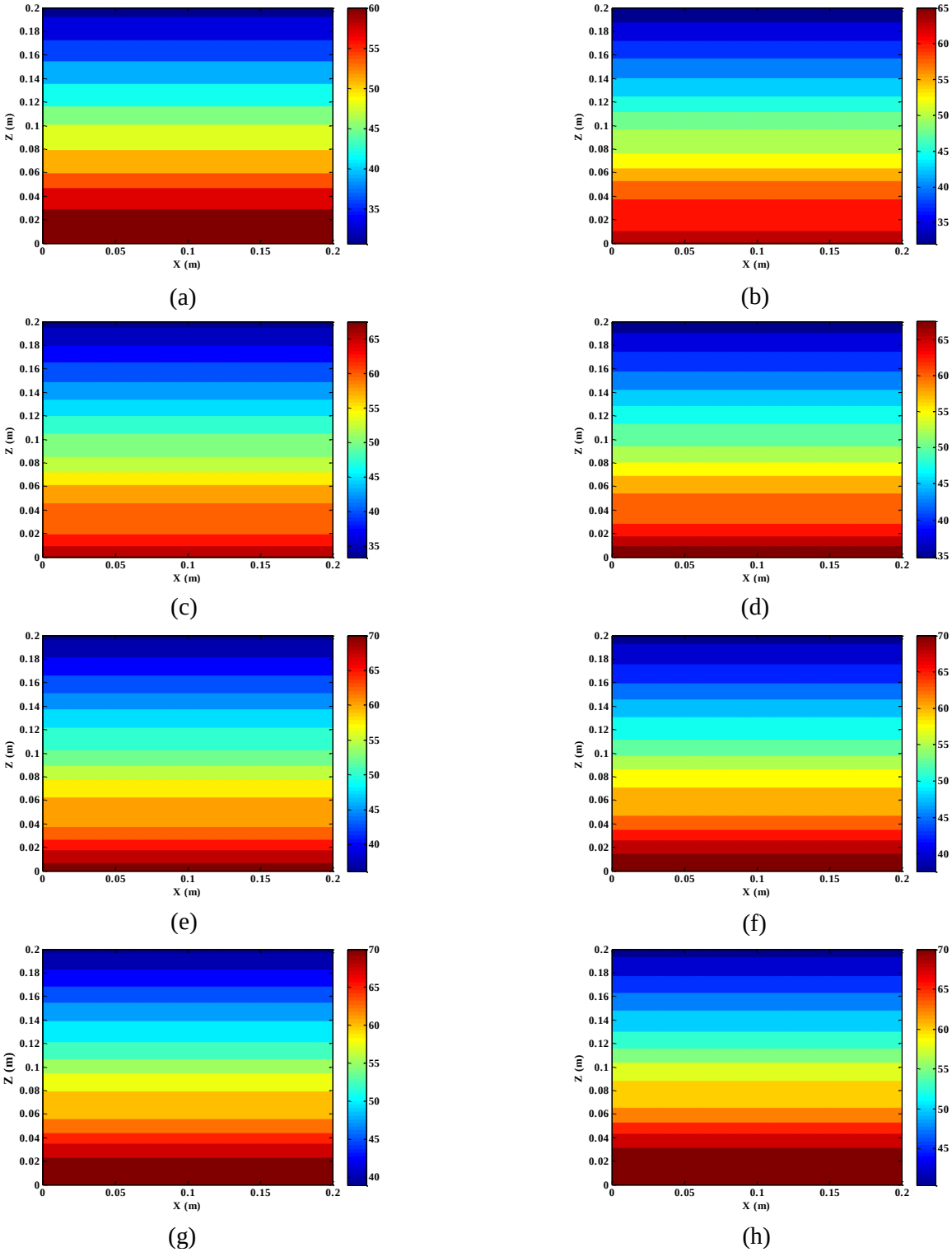

Figure 8. Temperature contours line for different time step when reaching steady state response with $a = 750\ W/m^2$, $\tau = 30s$, and$\Delta h = 10mm$: (a) $t = 0.125\tau$, (b) $t = 0.25\tau$, (c) $t = 0.375\tau$ (d) $t = 0.5\tau$, (e) $t = 0.625\tau$, (f) $t = 0.75\tau$, (g) $t = 0.875\tau$, (h) $t = \tau$.

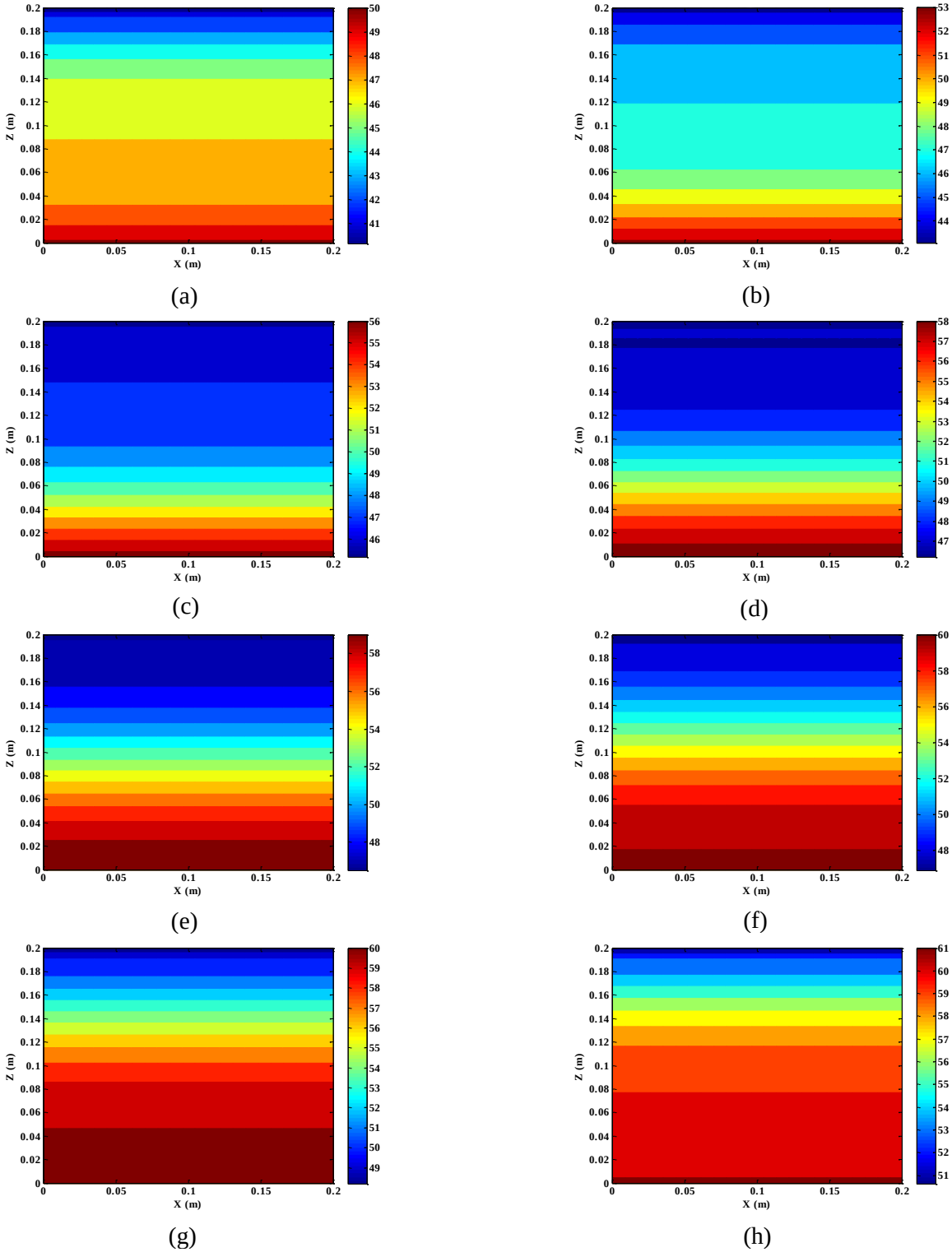

Figure 9. Temperature contours line for different time step when reacning steady state response with $a = 250\ W/m^2$, $\tau = 60s$, and $\Delta h = 20mm$: (a) $t = 0.125\tau$, (b) $t = 0.25\tau$, (c) $t = 0.375\tau$ (d) $t = 0.5\tau$, (e) $t = 0.625\tau$, (f) $t = 0.75\tau$, (g) $t = 0.875\tau$, (h) $t = \tau$.

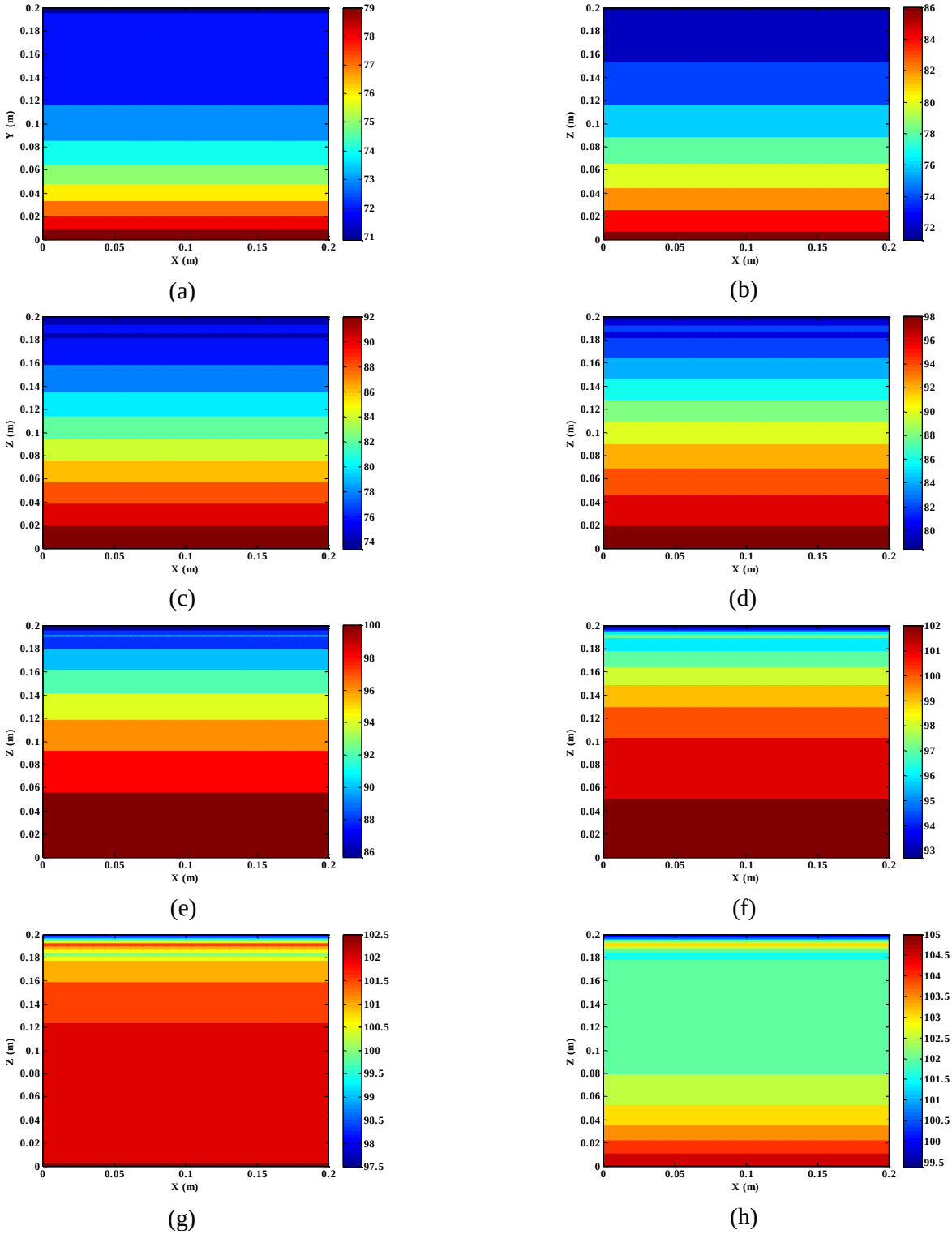

Figure 10. Temperature contours line for different time step when reaching steady state response with $a = 250\,W/m^2$, $\tau = 120s$, and $\Delta h = 20mm$: (a) $t = 0.125\tau$, (b) $t = 0.25\tau$, (c) $t = 0.375\tau$ (d) $t = 0.5\tau$, (e) $t = 0.625\tau$, (f) $t = 0.75\tau$, (g) $t = 0.875\tau$, (h) $t = \tau$.

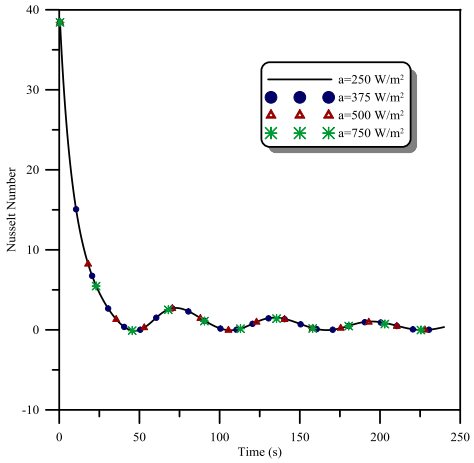

Figure 11. Average Nusselt number versus time for different amplitude, $\Delta h = 10\ mm$ and $\tau = 60\ s$.

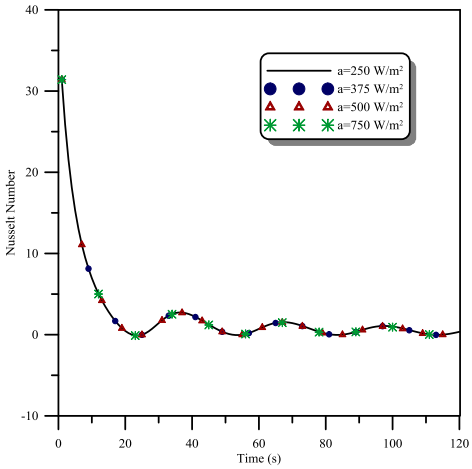

Figure 12. Average Nusselt number versus time for different amplitude, $\Delta h = 20\ mm$ and $\tau = 30\ s$.

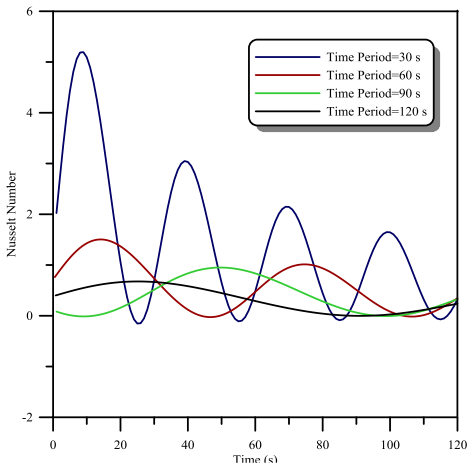

Figure 13. Average Nusselt number versus time at the last 120 $s, \Delta h = 10\ mm$ and $a = 375\ W/m^2$.

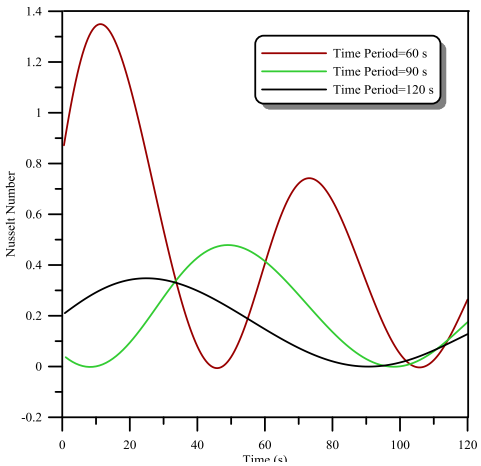

Figure 14. Average Nusselt number versus time at the last 120 s for $\Delta h = 20\ mm$ and $a = 250\ W/m^2$.

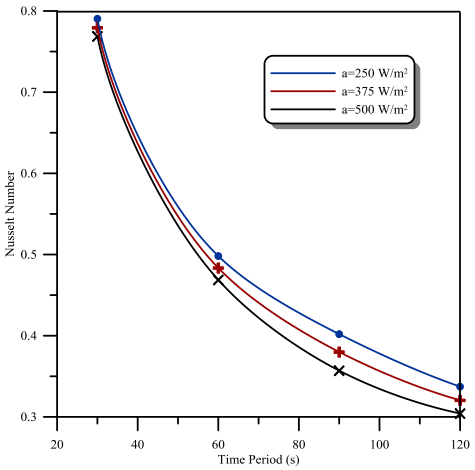

Figure 15. Time averaged Nusselt number variation with time period for different amplitude and $\Delta h = 10\ mm$.

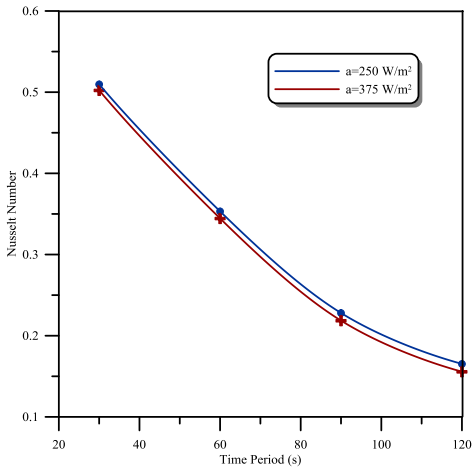

Figure 16. Time averaged Nusselt number variation with time period for different amplitude and $\Delta h = 20\ mm$.